

## Heterozygous loss-of-function *SMC3* variants are associated with variable and incompletely penetrant growth and developmental features

Morad Ansari<sup>1,2,39</sup>, Kamli N. W. Faour<sup>3,4,39</sup>, Akiko Shimamura<sup>5</sup>, Graeme Grimes<sup>2</sup>, Emeline M. Kao<sup>6</sup>, Erica R. Denhoff<sup>6</sup>, Ana Blatnik<sup>2,7</sup>, Daniel Ben-Isvy<sup>8,9,10</sup>, Lily Wang<sup>8,9,10</sup>, Benjamin M. Helm<sup>11</sup>, Helen Firth<sup>12</sup>, Amy M. Breman<sup>11</sup>, Emilia K. Bijlsma<sup>13</sup>, Aiko Iwata-Otsubo<sup>11</sup>, Thomy J.L. de Ravel<sup>14</sup>, Vincent Fusaro<sup>15</sup>, Alan Fryer<sup>16</sup>, Keith Nykamp<sup>15</sup>, Lara G. Stühn<sup>17</sup>, Tobias B. Haack<sup>17</sup>, G. Christoph Korenke<sup>18</sup>, Panayiotis Constantinou<sup>19</sup>, Kinga M. Bujakowska<sup>20</sup>, Karen J. Low<sup>21,22</sup>, Emily Place<sup>20</sup>, Jennifer Humberson<sup>23</sup>, Melanie P. Napier<sup>24</sup>, Jessica Hoffman<sup>24</sup>, Jane Juusola<sup>24</sup>, Matthew A. Deardorff<sup>25</sup>, Wanqing Shao<sup>26</sup>, Shira Rockowitz<sup>26,27,3</sup>, Ian Krantz<sup>28</sup>, Maninder Kaur<sup>28</sup>, Sarah Raible<sup>28</sup>, Sabine Kliesch<sup>29</sup>, Moriel Singer-Berk<sup>9</sup>, Emily Groopman<sup>3,9</sup>, Stephanie DiTroia<sup>9</sup>, Sonia Ballal<sup>4,30</sup>, Siddharth Srivastava<sup>4,31</sup>, Kathrin Rothfelder<sup>32</sup>, Saskia Biskup<sup>32,33</sup>, Jessica Rzasz<sup>34</sup>, Jennifer Kerkhof<sup>34</sup>, Haley McConkey<sup>34</sup>, Anne O'Donnell-Luria<sup>3,8,9</sup>, Bekim Sadikovic<sup>34</sup>, Sarah Hilton<sup>35</sup>, Siddharth Banka<sup>35</sup>, Frank Tüttelmann<sup>36</sup>, Donald Conrad<sup>37,38</sup>, Michael E. Talkowski<sup>9,8</sup>, David R. FitzPatrick<sup>2,40</sup>, Philip M. Boone<sup>4,3,8,9,40,\*</sup>

<sup>1</sup>South East Scotland Genetic Service, Western General Hospital, Edinburgh, UK, <sup>2</sup>MRC Human Genetics Unit, Institute of Genetics and Cancer, University of Edinburgh, Edinburgh, UK, <sup>3</sup>Division of Genetics and Genomics, Boston Children's Hospital, Boston, MA, US, <sup>4</sup>Cornelia de Lange Syndrome and Related Disorders Clinic, Boston Children's Hospital, Boston, MA, US, <sup>5</sup>Division of Hematology and Oncology, Boston Children's Hospital, Boston, MA, US, <sup>6</sup>Institutional Centers for Clinical and Translational Research, Boston Children's Hospital, Boston, MA, US, <sup>7</sup>Department of Clinical Cancer Genetics, Institute of Oncology Ljubljana, Ljubljana, SI, <sup>8</sup>Center for Genomic Medicine, Massachusetts General Hospital, Boston, MA, US, <sup>9</sup>Medical and Population Genetics, The Broad Institute of MIT and Harvard, Cambridge, MA, US, <sup>10</sup>Division of Medical Sciences, Harvard Medical School, Boston, MA, US, <sup>11</sup>Department of Medical and Molecular Genetics, Indiana University School of Medicine, Indianapolis, IN, US, <sup>12</sup>Clinical Genetics, Addenbrooke's Hospital, Cambridge University Hospitals, Cambridge, UK, <sup>13</sup>Department of Clinical Genetics, Leiden University Medical Centre, Leiden, NL, <sup>14</sup>Centre for Human Genetics, UZ Leuven/ Leuven University Hospitals, Leuven, BE, <sup>15</sup>Invitae, San Francisco, CA, US, <sup>16</sup>Department of Clinical Genetics, Alder Hey Children's Hospital Liverpool, Liverpool, UK, <sup>17</sup>Institute of Medical Genetics and Applied Genomics, University of Tuebingen, Tuebingen, DE, <sup>18</sup>University Children's Hospital Oldenburg, Department of Neuropaediatric and Metabolic Diseases, University Children's Hospital Oldenburg, Oldenburg, DE, <sup>19</sup>West of Scotland Centre for Genomic Medicine, Queen Elizabeth University Hospital, Glasgow, UK, <sup>20</sup>Massachusetts Eye and Ear Infirmary, Boston, MA, US, <sup>21</sup>University Hospitals Bristol and Weston NHS Foundation Trust, Bristol, UK, <sup>22</sup>University of Bristol, Bristol, UK, <sup>23</sup>University of Virginia Health System, Charlottesville, VA, US, <sup>24</sup>GeneDx, Gaithersburg, MD, US, <sup>25</sup>Departments of Pathology and Pediatrics, Children's Hospital Los Angeles and University of Southern California, Los Angeles, CA, US, <sup>26</sup>Research Computing, Information Technology, Boston Children's Hospital, Boston, MA, US, <sup>27</sup>The Manton Center for Orphan Disease Research, Boston Children's Hospital, Boston, MA, US, <sup>28</sup>Children's Hospital of Philadelphia, Philadelphia, PA, US, <sup>29</sup>Department of Clinical and Surgical Andrology, Centre of Reproductive Medicine and Andrology, University Hospital Münster, Münster, DE, <sup>30</sup>Division of Gastroenterology, Boston Children's Hospital, Boston, MA, US, <sup>31</sup>Division of Neurology, Boston Children's Hospital, Boston, MA, US, <sup>32</sup>Zentrum für Humangenetik, Tübingen, DE, <sup>33</sup>Center for Genomics and Transcriptomics (CeGaT), Tübingen, DE, <sup>34</sup>Molecular Diagnostics Program and Verspeeten Clinical Genome Centre, LHSC, London, CA, <sup>35</sup>Manchester University, Manchester, UK, <sup>36</sup>Institute of Reproductive Genetics, University of Münster, Münster, DE, <sup>37</sup>Division of Genetics, Oregon National Primate Research Center, Oregon Health and Science University, Portland, OR, US, <sup>38</sup>Center for Embryonic Cell and Gene Therapy, Oregon Health and Science University, Portland, OR, US, <sup>39</sup>These authors contributed equally, <sup>40</sup>These authors contributed equally.

\*Correspondence:

Dr. Philip M. Boone

Cornelia de Lange Syndrome and Related Disorders Clinic

Boston Children's Hospital

300 Longwood Ave.

Boston, MA, USA 02115

Tel: +1 (617) 355-6394

E-mail: [philip.boone@childrens.harvard.edu](mailto:philip.boone@childrens.harvard.edu)

## 1 **Abstract**

2 Heterozygous missense variants and in-frame indels in *SMC3* are a cause of Cornelia  
3 de Lange syndrome (CdLS), marked by intellectual disability, growth deficiency, and  
4 dysmorphism, via an apparent dominant-negative mechanism. However, the spectrum of  
5 manifestations associated with *SMC3* loss-of-function variants has not been reported, leading  
6 to hypotheses of alternative phenotypes or even developmental lethality. We used  
7 matchmaking servers, patient registries, and other resources to identify individuals with  
8 heterozygous, predicted loss-of-function (pLoF) variants in *SMC3*, and analyzed population  
9 databases to characterize mutational intolerance in this gene. Here, we show that *SMC3*  
10 behaves as an archetypal haploinsufficient gene: it is highly constrained against pLoF  
11 variants, strongly depleted for missense variants, and pLoF variants are associated with a  
12 range of developmental phenotypes. Among 13 individuals with *SMC3* pLoF variants,  
13 phenotypes were variable but coalesced on low growth parameters, developmental  
14 delay/intellectual disability, and dysmorphism reminiscent of atypical CdLS. Comparisons to  
15 individuals with *SMC3* missense/in-frame indel variants demonstrated a milder presentation  
16 in pLoF carriers. Furthermore, several individuals harboring pLoF variants in *SMC3* were  
17 nonpenetrant for growth, developmental, and/or dysmorphic features, some instead having  
18 intriguing symptomatology with rational biological links to *SMC3* including bone marrow  
19 failure, acute myeloid leukemia, and Coats retinal vasculopathy. Analyses of transcriptomic  
20 and epigenetic data suggest that *SMC3* pLoF variants reduce *SMC3* expression but do not  
21 result in a blood DNA methylation signature clustering with that of CdLS, and that the global  
22 transcriptional signature of *SMC3* loss is model-dependent. Our finding of substantial  
23 population-scale LoF intolerance in concert with variable penetrance in subjects with *SMC3*  
24 pLoF variants expands the scope of cohesinopathies, informs on their allelic architecture, and

25 suggests the existence of additional clearly LoF-constrained genes whose disease links will  
26 be confirmed only by multi-layered genomic data paired with careful phenotyping.

27 **Keywords:** Cornelia de Lange syndrome, SMC3, loss-of-function, cohesin, CdLS3, LoF

## 28 **Introduction**

29           The cohesin complex, a multimeric structure with the ability to entrap DNA, is  
30 integral to several dynamic genome processes.<sup>1,2</sup> Specifically, cohesin facilitates sister  
31 chromatid cohesion during cell division,<sup>3</sup> DNA repair,<sup>4</sup> 3D chromatin architecture,<sup>5</sup> and  
32 transcriptional control of developmental genes.<sup>6,7</sup> SMC3 (structural maintenance of  
33 chromosomes 3), the sole subunit shared by mitotic, interphase, and meiotic cohesin, is a  
34 ubiquitously expressed protein that binds with SMC1A/B to form the legs of the isosceles  
35 triangle commonly used to represent the closed heterotrimeric cohesin ‘ring,’ with  
36 RAD21/REC8 forming the base.

37           In mouse models, homozygous *SMC3* loss<sup>8,9</sup> or conditional *SMC3* depletion in  
38 oocytes<sup>10</sup> results in embryonic lethality. In embryonic and adult mice, homozygous *SMC3*  
39 loss in the blood compartment causes myeloid-based hematopoietic failure.<sup>11,12</sup> However,  
40 *SMC3* heterozygosity in mice is tolerated and associated with behavioral phenotypes,  
41 neuronal/synaptic differences in the cerebral cortex, decreased body weight, craniofacial  
42 dysmorphism, and changes in gene expression,<sup>8,9</sup> suggesting the potential for a similar  
43 phenomenon in humans.<sup>13</sup>

44           Missense variants and in-frame indels in *SMC3* have been identified among patients  
45 with mild/atypical Cornelia de Lange syndrome (CdLS).<sup>13-15</sup> Typical (classic) CdLS is caused  
46 by constitutional or mosaic heterozygous loss-of-function (LoF) pathogenic variants in  
47 *NIPBL* and is distinguished from atypical CdLS, which is a spectrum, by greater overall  
48 severity with a more characteristic facial appearance and the presence of major  
49 malformations. Variable intellectual disability, behavioral abnormalities, hirsutism, growth  
50 failure, gastroesophageal dysfunction, and short first metacarpals are seen in both typical and  
51 atypical cases. *SMC3*-related CdLS is principally marked by intellectual disability, facial  
52 dysmorphism, microcephaly, and postnatal growth delay.<sup>13-16</sup>

53           The reported missense variants and in-frame indels in *SMC3* generally fall within  
54 important protein regions including the antiparallel coiled-coil, hinge, and head domains.<sup>14</sup>  
55 Tested pathogenic variants appear to act as dominant-negative alleles in human cell lines,  
56 where they increase the affinity of SMC hinge dimers for DNA, promoting genome  
57 instability and impairing genomic spatial organization.<sup>17</sup> *In silico* modeling is also consistent  
58 with a dominant-negative effect.<sup>14</sup> Furthermore, proteomic analyses reveal that missense-  
59 mutated *SMC3* proteins are incorporated into the cohesin complex normally but prompt  
60 dysregulation of the c-MYC transcription factor, a feature of CdLS in the early prenatal  
61 period.<sup>18</sup> Finally, *SMC3* missense variants in CdLS patients confer a DNA methylation  
62 episignature grouping with that of other CdLS genes.<sup>19</sup>

63           There is considerable importance of allele type in other cohesin genes, for example  
64 *NIPBL* (missense in mild CdLS vs LoF in severe CdLS<sup>20-22</sup>) and *SMC1A* (missense in  
65 atypical CdLS vs LoF in *SMC1A*-related developmental and epileptic encephalopathy<sup>23</sup>).  
66 Thus, it has been proposed that the absence of *SMC3* predicted LoF (pLoF) variants in  
67 previously described CdLS cases could be due to those variants either causing a different  
68 phenotype or being lethal for the developing embryo.<sup>24</sup> Somatic *SMC3* pLoF variants have  
69 been found in myeloid malignancies,<sup>25</sup> including acute myeloid leukemia<sup>26</sup> and Down  
70 syndrome acute megakaryoblastic leukemia.<sup>27,28</sup> This is in line with LoF alleles in cohesin  
71 genes being a common event in several tumor types, not as initiating events but as subsequent  
72 drivers.<sup>29</sup> Population genetic data suggest that germline *SMC3* pLoF variants are considerably  
73 depleted           in           the           general           population  
74 (<https://gnomad.broadinstitute.org/gene/ENSG00000108055>); however, the consequence of  
75 heterozygous germline pLoF variants in humans is unknown, as only a single case is  
76 documented in the literature.<sup>15</sup>

77 Here, we describe the clinical phenotypes of 13 individuals with germline pLoF  
78 variants in *SMC3*, including four frameshifts, four stop gains, four deletions, and one  
79 predicted damaging splice variant. Many, but not all, individuals have developmental delay,  
80 low growth parameters, and/or mild dysmorphism – reminiscent of atypical CdLS.  
81 Comparisons of quantitative growth and developmental data between pLoF carriers and  
82 published cases of *SMC3* pathogenic missense variants and in-frame indels reveal a  
83 genotype-phenotype correlation, with pLoF conferring milder – albeit overlapping –  
84 parameters. We also observe several individuals without growth or neurodevelopmental  
85 abnormalities and test multiple hypotheses to explain this incongruity. Our findings suggest  
86 that a broader class of undiscovered Mendelian conditions stemming from LoF variants in  
87 highly constrained genes likely remains uncatalogued owing to generic, variable, and/or  
88 incompletely penetrant phenotypes and will require large dataset analyses, deep phenotyping,  
89 and functional experimentation to solve.

## 90 **Subjects and Methods**

### 91 *Case recruitment*

92 Anonymized genetic and phenotypic information was collected, subjects were  
93 enrolled, and database searches performed under Boston Children’s Hospital IRB-approved  
94 protocol #00040134. Multiple sources were queried to identify individuals with predicted  
95 loss of function variants in *SMC3*: ClinVar (<https://www.ncbi.nlm.nih.gov/clinvar/>);<sup>30</sup>  
96 GeneMatcher/Matchmaker Exchange (<https://genematcher.org/>);<sup>31</sup> the Baylor Genetics,  
97 GeneDx, Indiana University School of Medicine Genetic Testing, and Invitae clinical  
98 laboratories; a database of patients at Boston Children’s Hospital;<sup>32</sup> an in-house data portal  
99 built upon seqr<sup>33</sup> and drawing from the Broad Institute Center for Mendelian Genomics and  
100 GREGoR Consortium projects; DECIPHER (<https://www.deciphergenomics.org/>);<sup>34</sup> and one

101 previously-published individual with an *SMC3* nonsense variant referred for routine CdLS  
102 screening due to CdLS-like features and developmental delay.<sup>15</sup>

### 103 *Growth and developmental milestone comparisons*

104 Growth measurements were converted to Z-scores using the British Growth Survey  
105 data (<https://www.rcpch.ac.uk/resources/growth-charts>). Statistical comparisons and plot  
106 generation were undertaken using R.

### 107 *Subject variant identification*

108 Variants were identified via exome sequencing, microarray, or gene panel. These  
109 methods are listed for each case in Table S1, as is the confirmation status of variants by  
110 orthogonal methods.

### 111 *Gene annotations*

112 RefSeq transcript NM\_005445 (Gencode ENST00000361804.5), via  
113 (<https://genome.ucsc.edu/>) was used as the gene model for analyses. The Ensembl Variant  
114 Effect Predictor (<https://useast.ensembl.org/Tools/VEP>) was used to corroborate subjects'  
115 variant nomenclature. Regional missense constraint for *SMC3* was based on gnomAD data  
116 and assessed at a threshold of  $p=0.001$  as in  
117 <https://www.biorxiv.org/content/10.1101/148353v1> and <sup>35</sup>. The region of potential escape  
118 from nonsense mediated decay was considered as the final 55 nt of the penultimate exon of  
119 *SMC3* (codon 1176 and beyond). GRCh38/hg38 is the default genome build used unless  
120 specified otherwise.

### 121 *UK Biobank pLoF sequence variant curation*

122 The 10-110575403-TGTGA-T splice site variant, present in 5 individuals in the  
123 UKBB, was removed from the list of *SMC3* pLoF variants in UKBB; this is on account of it  
124 not resulting in an alteration to the first 5 nt of the 5' splice site.

#### 125 *Copy-number variant detection among UK Biobank samples*

126 UKBB *SMC3* deletions were called using GATK-gCNV with genomic interval  
127 selection, sample processing, and defragmentation performed as in  
128 (<https://www.biorxiv.org/content/10.1101/2022.08.25.504851v1>). In brief, exome sequencing  
129 reads were first mapped to a predefined set of genomic intervals curated to capture the exonic  
130 regions of canonical protein-coding genes, and coverage was collected across well-captured  
131 intervals for copy number (CN) inference. Samples with similar global read depth profiles  
132 were then clustered into batches to be jointly processed by GATK-gCNV, which outputs  
133 CNV calls across the set of well-captured intervals. These raw calls were subsequently  
134 defragmented, and to ensure that calls were not merged across high-quality CN=2 regions,  
135 CNVs were refragmented to preserve any CN=2 segments spanning at least 3 exome  
136 sequencing probes with quality score (QS)  $\geq 100$ . Finally, the resulting callset was refined  
137 using the recommended QS, sample-level, and site frequency filters from  
138 (<https://www.biorxiv.org/content/10.1101/2022.08.25.504851v1>) along with a filter to  
139 remove CNVs covering fewer than 3 exons.

#### 140 *Infertility cohort missense burden analysis*

141 Comparisons were made to gnomAD v2.1.1 missense *SMC3* variants with CADD  
142 score  $>25$  (Table S4) as assigned by the Variant Effect Predictor  
143 (<https://useast.ensembl.org/info/docs/tools/vep/index.html>). The cumulative allele frequency  
144 was transformed to a fraction with a denominator representing the mean number of alleles  
145 across these variants, for the purpose of chi-square analysis.



146 *Gene expression analyses*

147 *SMC3* gene expression data were derived from Cancer Cell Line Encyclopedia  
148 (CCLE) samples, restricted to hematopoietic and lymphoid tumors, obtained via  
149 (<http://xenabrowser.net>). Nonsense, frameshift, or splice site variants were considered  
150 predicted loss-of-function (pLoF). Samples containing >1 *SMC3* variant were categorized by  
151 the most damaging variant class. Samples solely containing missense or silent *SMC3* variants  
152 were removed, as were samples lacking *SMC3* genotype or expression data.

153 Perturb-seq data were derived from Replogle et al.<sup>36</sup> and obtained via  
154 ([https://plus.figshare.com/articles/dataset/ Mapping\\_information-rich\\_genotype-  
155 phenotype\\_landscapes\\_with\\_genome-scale\\_Perturb-seq\\_Replogle\\_et\\_al\\_2022\\_-  
156 commonly\\_requested\\_supplemental\\_files/21632564/1](https://plus.figshare.com/articles/dataset/Mapping_information-rich_genotype-phenotype_landscapes_with_genome-scale_Perturb-seq_Replogle_et_al_2022_-_commonly_requested_supplemental_files/21632564/1)) and (<https://gwps.wi.mit.edu/>).

157 Briefly, this Perturb-seq experiment involved single-cell sequencing following pooled,  
158 multiplexed CRISPR interference (CRISPRi) in three parallel approaches, each using a  
159 different CRISPRi guide library: K562 (chronic myelogenous leukemia, female) cells  
160 receiving a genome-wide guide library against all expressed genes and harvested on day 8  
161 after transduction; K562 cells receiving a DepMap essential gene guide library and harvested  
162 on day 6 after transduction; and hTERT RPE1 (retinal pigment epithelium, female) cells  
163 receiving a DepMap essential gene guide library and harvested on day 7 after transduction.  
164 Each library vector construct encoded two guides (sgRNAs) per target gene.

165 *Smc3*<sup>+/-</sup> mouse cortex differentially expressed genes from RNA sequencing were  
166 obtained from Fujita et al.<sup>8</sup> *Nipbl*<sup>+/-</sup> whole brain RNA sequencing data were obtained from  
167 Kean et al.<sup>37</sup> In comparisons of these datasets, a denominator of 30,686 genes (see Fig. 3d)  
168 was established from among the 55,228 total genes mapped in Kean et al.<sup>37</sup> (GEO entry:  
169 <https://www.ncbi.nlm.nih.gov/geo/query/acc.cgi?acc=GSE203014>) based on those having 10  
170 or more reads across all 22 samples, which was the cutoff used in the original analysis.

171 Statistical analyses were conducted in R. Key gene lists are in Table S5.

#### 172 *DNA methylation analysis*

173 DNA from blood was subjected to array-based methylation analysis via the  
174 Manchester EpiPro project ([https://mft.nhs.uk/nwglh/test-information/rare-disease/epipro-  
175 project/](https://mft.nhs.uk/nwglh/test-information/rare-disease/epipro-project/)). The genome-wide DNA methylation profile was compared to the EpiSign  
176 Knowledge Database, a collection of DNA methylation signatures specific for rare disorders,  
177 as in Aref-Eshghi et al.<sup>19</sup>

## 178 **Results**

### 179 *Case series and subject phenotypes*

180 Thirteen individuals with *SMC3* predicted loss of function (pLoF) variants were  
181 identified. Most subjects underwent genetic testing as part of routine clinical assessment for  
182 growth retardation, developmental delay, and/or dysmorphic features. In only three cases was  
183 there clinical suspicion of CdLS. Some cases were identified via diagnostic laboratories,  
184 research repositories, hospital-based databases, and GeneMatcher. Subjects possessed  
185 frameshift indel, deletion, stop gain, or splice variants (Tables 1, S1; Fig. 1). Of these 13  
186 variants, five were *de novo*, one was maternally inherited, two were paternally inherited, and  
187 six were of unknown inheritance. Adjudication of the nine SNVs using an advanced LoF  
188 curation framework (<https://www.medrxiv.org/content/10.1101/2023.03.08.23286955v1>)  
189 flagged two as potentially not having a LoF effect (one splice variant and one escape from  
190 nonsense mediated decay) (Table S1). Missense variants were specifically excluded, as  
191 missense variant effects (e.g., hypomorphic vs nullimorphic vs dominant negative) are unable  
192 to be reliably predicted.

193 Information on individual patients' clinical features can be acquired by contacting the  
194 corresponding authors. This information will be included in a future peer-reviewed

195 manuscript but is prohibited by medRxiv. No feature was shared by all subjects, however the  
196 features present in more than half of subjects included developmental delay and/or  
197 intellectual disability, low growth, and facial dysmorphism. The majority of the typical CdLS  
198 facial features and associated malformations were rare or absent in our patient cohort. No low  
199 anterior hairline or major limb malformations were reported. Only two individuals had a  
200 long/featureless philtrum, one had ptosis, three had confirmed dental anomalies, and one had  
201 downturned corners of the mouth. Three individuals had synophrys, three had arched  
202 eyebrows, and five had long eyelashes. Three individuals had brachycephaly, three had a thin  
203 upper lip, and three had a depressed nasal bridge. Four individuals had cardiac  
204 malformations, and two experienced gastroesophageal reflux (GER). Hirsutism was  
205 described in three cases. Interestingly, five out of thirteen individuals had a degree of  
206 micrognathia/retrognathia. Intellectual disability was present in four individuals and learning  
207 disability in an additional one. A delay in reaching developmental milestones was detected in  
208 nine individuals. Autistic features were present in three individuals. Photographs were not  
209 available for any subject with dysmorphic features.

210 We compared standardized postnatal growth parameters and age at reaching  
211 developmental milestones between carriers of *SMC3* pLoF variants and 15 cases with  
212 pathogenic missense variants or in-frame indels in *SMC3* as previously published.<sup>14</sup> A  
213 difference in standardized birth weight, birth head circumference, postnatal (i.e. at time of  
214 enrollment) weight, and postnatal head circumference was detected between the two groups,  
215 pLoF variants being associated with less pronounced growth delay than missense/in-frame  
216 indel variants, however these differences did not reach a significance threshold of  $p \leq 0.05$   
217 (Fig. 2a). When comparing the age at achieving developmental milestones, the patients with  
218 pLoF variants were able to sit unaided, walk unaided, and speak at a younger age than  
219 patients with missense/in-frame indels, although only the difference in age at sitting was

220 significant ( $p=0.023$ ) (Fig. 2b). pLoF subjects' growth and developmental milestones were  
221 each delayed compared with the population mean in growth and developmental data (Fig. 2).  
222 Thus, in general *SMC3* pLoF variants are associated with a milder phenotype than are  
223 missense variants; however, the spectra are variable and appear to overlap.

224 Interestingly, several subjects had other phenotypes with potential biological links to  
225 *SMC3* (see Discussion) including bone marrow failure or leukopenia, acute myeloid leukemia  
226 (AML), and Coats retinal telangiectasis, however these were limited to a single case each.  
227 Additional phenotypic and laboratory details, where available, are in the Supplemental Note.

#### 228 *SMC3* mutational constraint

229 We were intrigued by subjects who were nonpenetrant for, or had mild presentations  
230 of, the above growth and developmental phenotypes given initial metrics suggesting  
231 mutational intolerance in this gene. Thus, we sought to further characterize LoF constraint in  
232 *SMC3*. Consistent with *in vitro*<sup>38,39</sup> and model organism studies<sup>9,10,40,41</sup> indicating *SMC3* is an  
233 essential developmental gene, biallelic pLoF variants have never been described in a human  
234 being, including our cases.

235 Regarding heterozygous variants, the gnomAD v2.1.1  
236 (<https://gnomad.broadinstitute.org/>) probability of LoF intolerance (pLI) score (evidence for  
237 depletion of functional variation from expectation within each gene) and the loss-of-function  
238 observed/expected upper bound fraction (LOEUF; a more continuous metric that directly  
239 measures the ratios of observed to expected variation) both place *SMC3* among the group of  
240 genes predicted to be most highly intolerant to LoF variants in a population cohort of adults  
241 without severe pediatric disease (pLI = 1; expected/observed ratio of SNV pLoF variants  
242 passing filters = 79.5/0; LOEUF 0.04).<sup>42</sup> In agreement with this, an estimation of the  
243 probability of haploinsufficiency (pHaplo) of *SMC3* based on a machine learning model  
244 trained on a broad case-control CNV burden analysis in >950,000 individuals and gene-level

245 features was 0.998 (max score = 1.00);<sup>43</sup> of interest, the probability of triplosensitivity  
246 (pTriplo) is also very high (0.999). A review of multiple additional databases of control and  
247 affected subjects revealed rarity and considerable apparent selection against such alleles  
248 (Table S2): No pLoF structural variants are present in gnomAD-SV, and our own CNV  
249 analysis of UK Biobank (UKBB) exome data identified only two deletions involving *SMC3*  
250 among 196,869 subjects (Fig. S2). pLoF sequence and structural variants are similarly rare or  
251 absent in the Database of Genomic Variants (DGV) and DECIPHER (Table S2).

252 To gain insights into the few heterozygous *SMC3* pLoF SNV carriers in control  
253 populations, who would presumably be nonpenetrant or mildly affected, we cataloged these  
254 alleles in gnomAD and the UK Biobank (UKBB) (Fig. 1a; Table S3). The overall frequency  
255 of pLoF variants in gnomAD is 6.37E-5 (1/15,699) and in UKBB is 3.32E-5 (1/30,102), and  
256 all are singletons. There was neither a strong indication of mosaicism (e.g., low allele  
257 balance) nor an age-dependent increase in allele frequency suggestive of clonal  
258 hematopoiesis among gnomAD pLoF variants (Fig. S1). Adjudication of the nine gnomAD  
259 pLoF variants using the LoF curation framework described above flagged two as not having a  
260 LoF effect and an additional two as uncertain or potential technical artifacts (e.g.,  
261 homopolymer repeat region, lack of read data) (Table S3).

262 Mapping case pLoF SNVs to the *SMC3* coding sequence suggested possible  
263 clustering toward the 5' half of the transcript (Fig. 1a). To identify gene-level features that  
264 would support the veracity and/or biological meaning of such a cluster, we first referenced  
265 GTEx (<https://gtexportal.org/home/gene/SMC3>) and found that the full-length, canonical  
266 transcript is the only isoform expressed at an appreciable level in any adult human tissue  
267 (Fig. 3a). Further supporting this being the sole isoform, normalized by-exon expression as  
268 measured by pext<sup>44</sup> (obtained via gnomAD) was homogeneous (score=1) across all exons in  
269 every GTEx tissue. Next, we investigated whether the existence of *SMC3PI*, a homologous

270 pseudogene at 2q11.2 that is likely the result of retrotransposition of approximately the last 5  
271 exons of *SMC3* (Fig. 1a), might be impairing variant mapping in that region resulting in an  
272 artifactual depletion of 3' variants. However, per-base mean depth of coverage among  
273 gnomAD exomes and genomes is similar across the entirety of *SMC3*  
274 ([https://gnomad.broadinstitute.org/gene/ENSG00000108055?dataset=gnomad\\_r2\\_1](https://gnomad.broadinstitute.org/gene/ENSG00000108055?dataset=gnomad_r2_1)), and  
275 *SMC3* pLoF variants in gnomAD/UKBB (Fig. 1a) and somatic *SMC3* pLoF variants in  
276 tumors from the NCI GDC collection (Fig. 1b) show an even spread across the gene. Finally,  
277 we calculated regional missense constraint scores across *SMC3* (Fig. 1c); while constraint  
278 scores are slightly higher at the 5' end, the entire gene is substantially missense constrained  
279 ( $o/e = 0.28$  ( $0.25 - 0.32$ );  $Z=6.4$ ). These data argue against any meaningful clustering of pLoF  
280 SNVs.

#### 281 *Potential explanations for mild phenotypes and nonpenetrance*

282 Having made a strong case for intolerance to heterozygous LoF of *SMC3*, we  
283 continued to seek to explain cases with mild or nonpenetrant developmental and/or growth  
284 phenotypes. One potential explanation is mosaicism. Thus, we assessed inheritance and allele  
285 balance among our enrolled cases. Variants were inherited in three cases and thus by  
286 definition germline mutations in those probands. No case variants were signed out by clinical  
287 labs as having allele fractions suggestive of mosaicism. Furthermore, in one subject lacking  
288 growth or developmental delay, we identified the mutant allele in three separate tissues (bone  
289 marrow, skin biopsy, and blood) with a near-50% allele balance (Supplemental Note).

290 Another potential explanation for mildly- or un-affected individuals with variants in  
291 considerably haploinsufficient genes is that they are dominant infertility/subfertility genes.  
292 Indeed, testis and ovary are the adult human tissues with highest relative expression of *SMC3*  
293 (<https://gtexportal.org/home/gene/SMC3>). Yet, *SMC3* has never been identified as a human  
294 infertility gene, including the most recent large study of primary ovarian insufficiency,<sup>45</sup> and

295 we identified one maternally transmitted *SMC3* pLoF variant. We tested an alternative  
296 hypothesis that heterozygous LoF of *SMC3* might cause male infertility. We evaluated WES  
297 data from >1,000 individuals with non-obstructive azoospermia (NOA) in the GEMINI Phase  
298 I cohort<sup>46</sup> and >1200 additional exomes in a Phase II cohort (some of which were  
299 normozoospermic male controls and female infertility cases). No *SMC3* pLoF variants and  
300 only one missense variant with CADD score  $\geq 25$  were identified (Table S4). Additionally,  
301 we assessed rare (gnomAD MAF <1%) coding variants in the Male Reproductive Genomics  
302 (MERGE) cohort,<sup>47</sup> consisting of 2,100 exomes of infertile men with severe oligo-, crypto- or  
303 azoospermia. One pLoF and three missense variants with CADD  $\geq 25$  were identified (Table  
304 S4). MERGE missense variants were not enriched when compared with gnomAD variants  
305 with CADD  $\geq 25$  ( $p=0.612$ , 2-sample chi-squared test with continuity correction). Finally,  
306 among our cases were two paternally inherited variants.

### 307 *Functional effect*

308 We next sought to determine whether pLoF *SMC3* variants act as true LoF alleles and  
309 have broader functional genomic effects. As subject cell lines and RNA were not available,  
310 pLoF *SMC3* variants were identified among hematopoietic and lymphoid tumors from the  
311 Cancer Cell Line Encyclopedia (CCLE) with available RNA sequencing data; these led to a  
312 significant decrease in *SMC3* gene expression compared to tumors wild-type for *SMC3*  
313 ( $p=0.019$ , Mann-Whitney U test) (Fig. 3b).

314 To determine whether decreasing *SMC3* expression is likely to effect a molecular  
315 (transcriptomic) signature and to what extent this matches that of other CdLS/cohesinopathy  
316 genes, we analyzed Perturb-seq data from Replogle et al<sup>36</sup>. This resource employed  
317 multiplexed CRISPR interference followed by single cell RNA-sequencing. In a genome-  
318 wide experiment in K562 chronic myelogenous leukemia cells, cells receiving *SMC3*-  
319 targeting guide RNAs reduced *SMC3* expression to 68.5% residual and exhibited a

320 transcriptomic signature of several hundred up- and down-regulated genes (Table S6). The  
321 expression profile of *SMC3* knockdown was highly correlated with the knockdown profiles  
322 of other cohesin ring components (*SMC1A*, *RAD21*, *STAG2*) and the cohesin loading  
323 machinery (*NIPBL*, *MAU2*) (Fig. 3e). This correlation held true in separate Perturb-seq  
324 experiments targeting only essential genes in K562 or retinal pigment epithelium (RPE1)  
325 cells (Fig. S3). The data were also able to show a threshold above which *SMC3* knockdown –  
326 despite cohesin being involved in chromosome segregation – does not result in chromosome  
327 instability, similar to other cohesin genes (Table S6) and previous studies involving *SMC3*.<sup>48</sup>

328 *Smc3*<sup>+/-</sup> mice were previously shown to possess differences in P1-21 cortical gene  
329 expression,<sup>8</sup> in addition to behavioral differences. Despite substantial methodologic  
330 differences – for example age at tissue harvest, which is associated with significant changes  
331 in cohesin level<sup>8</sup> – we ventured to compare these differentially expressed genes to those  
332 observed in a study of E17.5 *Nipbl*<sup>+/-</sup> mouse whole brain, a model of typical CdLS.<sup>37</sup> No  
333 significant overlap was observed (Fig. 3c).

334 Finally, we sought to determine whether *SMC3* pLoF variants result in changes to the  
335 epigenome matching those of previously-described subjects with CdLS including individuals  
336 with missense and in-frame indel variants in *SMC3*, although largely driven by other CdLS  
337 genes.<sup>19</sup> Methylation analysis of blood DNA from one available subject (p.Arg360Ter) did  
338 not match that episinature (Fig. 4).

## 339 Discussion

340 While heterozygous *SMC3* missense and in-frame indel variants are a cause of  
341 atypical Cornelia de Lange syndrome (CdLS), and somatic *SMC3* predicted loss-of-function  
342 (pLoF) variants are found in cancers, the consequence of germline *SMC3* LoF variants in



343 humans has remained solely in the realm of speculation. The present study was aimed at  
344 resolving this question.

#### 345 *Clinical phenotype*

346 The *SMC3* pLoF cases presented here demonstrate that this variant type also  
347 contributes to a disease phenotype. Published *SMC3* missense and in-frame indel cases with  
348 atypical CdLS demonstrate growth retardation, developmental delay, and characteristic facial  
349 features.<sup>14</sup> We found that pLoF patients share these features, although by quantitative  
350 comparisons appear on average to have a milder – although overlapping – phenotype than  
351 those with missense/in-frame indel variants and would for the most part not be considered to  
352 have CdLS, which might explain the near-absence of *SMC3* pLoF variants among previously  
353 sequenced CdLS cohorts (Fig. 5). Furthermore, the phenotype is variable, with some subjects  
354 showing more severe growth or developmental delays and others being nonpenetrant for  
355 these key features. Of note, *Smc3*<sup>+/-</sup> mice have demonstrated neuronal, behavioral, growth,  
356 and craniofacial features.<sup>8,9</sup>

357 The pathogenesis of CdLS in previously-reported *SMC3* missense/in-frame cases has  
358 been suggested to be dominant negative, involving aberrant pairing of mutant *SMC3* with  
359 other components of the cohesin ring.<sup>17,18</sup> Our data suggest that, by contrast, a relative  
360 shortage of *SMC3* has a less severe impact on cohesin function, which suggests that allele-  
361 specific therapy to knock down dominant negative alleles – even completely – should be  
362 further explored. Nullimorphic and hypomorphic *SMC3* missense variants likely also exist  
363 and will be identified as such with further study (Fig. 5).

#### 364 *Deletions involving SMC3*

365 In the four patients with deletions at 10q25.2, *SMC3* is not the only gene involved in  
366 the rearrangement (Fig. 1d) and it is therefore possible that haploinsufficiency for other genes

367 in the region is causative for some aspects of their phenotype. A small number of genes in  
368 these intervals have been associated with dominant human disease, among which only  
369 heterozygous *SHOC2* and *SMC3* pathogenic variants cause dysmorphic features and  
370 developmental delay; however, the only known pathogenic *SHOC2* variant which causes  
371 Noonan-like syndrome with loose anagen hair (OMIM #607721) is missense. Previously  
372 reported 10q25.2 deletions detected by cytogenetic methods do not seem to be associated  
373 with CdLS-like facial features.<sup>49,50</sup>

374 Missense variants in *RBM20*, which is deleted in all four deletion cases, are associated  
375 with a form of dilated cardiomyopathy.<sup>51</sup> No patients in our study with deletions  
376 encompassing *RBM20* had any sign of cardiomyopathy. The small deletion which only  
377 contains *SMC3* and *RBM20* in one subject was of particular interest, as it was also detected in  
378 the subject's father who was reported to be healthy with no mention of heart disease.

### 379 *Potential explanations for mild/nonpenetrant cases despite LoF constraint*

380 Analyses of multiple population genomic analyses suggested that *SMC3* is  
381 substantially LoF-, missense-, and even duplication-constrained. Given substantial LoF  
382 constraint, it was then potentially surprising that we identified some individuals as having  
383 milder features as well as pLoF individuals in gnomAD and UKBB (albeit at a low allele  
384 frequency). Of note, constraint metrics are indicative of overall selective pressure rather than  
385 observable phenotypic severity,<sup>52</sup> and the above scenario has been described for other,  
386 similarly LoF-constrained disease genes (e.g. *ASXL3*, *ARID1B* and *AUTS2*).<sup>53</sup> Nonetheless,  
387 we sought to investigate potential alternative explanations:

388 Obligatory postzygotic mosaicism is seen in disorders for which germline pathogenic  
389 variation is lethal.<sup>54</sup> Mosaicism restricted to the blood lineage may be related to clonal  
390 hematopoiesis in aging,<sup>55</sup> which can be caused by somatic variants in a number of cohesin  
391 and related genes (e.g. *RAD21*, *SMCIA*, *STAG2*, *CTCF*)<sup>56</sup>. However, somatic *SMC3*

392 pathogenic variants have not previously been associated in isolation with clonal  
393 hematopoiesis,<sup>12</sup> and we found no evidence for mosaicism in our cases or in the few pLoF  
394 variants in gnomAD.

395 In mice, sufficient SMC3 protein is required in oocytes for early embryonic  
396 development,<sup>10</sup> and heterozygous depletion of *SMC3* in female mice has deleterious impacts  
397 on both the integrity and transmission of zygotic chromosomes.<sup>9,10,12</sup> Furthermore,  
398 conditional knockout of *HDAC8*, an SMC3 recycling factor, causes subfertility.<sup>57</sup> Finally,  
399 several cohesin or cohesin-related genes have been implicated in infertility in humans (*REC8*,  
400 *SMC1B*, *STAG3*, *SGO2*).<sup>58</sup> Yet, there is no published evidence of *SMC3* being involved in  
401 female infertility and our own analyses identified only rare *SMC3* pLoF variants among male  
402 infertility (azoospermia) cases and no statistical enrichment of predicted damaging missense  
403 variants.

#### 404 *Case-control phenotype associations*

405 *SMC3* deletions or pLoF (frameshift, stop gain, splice site) variants have not  
406 previously been found to be associated with disease in large case-control studies. For  
407 example, there were no control deletions or case deletions <1Mb in a large study generating a  
408 copy-number variant ‘morbidity map’ of individuals with developmental delay,<sup>59</sup> and only  
409 one protein truncating variant (included in the present manuscript) was found among DDD  
410 study data.<sup>60</sup> The UK Biobank (UKBB) demonstrates only one moderately significant  
411 phenotypic association for pLoF variants (mean corpuscular volume)  
412 (<https://app.genebase.org/gene/ENSG00000108055>)<sup>61</sup>. Intriguingly, in an analysis of >31k  
413 individuals with neurodevelopmental phenotypes and their family members, *de novo* variants  
414 in *SMC3* were found to be associated with developmental delay (false discovery rate = 3.46E-  
415 7), although driven mostly by missense variants.<sup>62</sup> The lack of phenotypic associations with

416 *SMC3* pLoF variants in large cohorts could be on account of a lack of true association and/or  
417 lack of power owing to the rarity of these variants.

418 *The possibility of pleiotropic phenotypes*

419 Several patients had intriguing ‘other’ phenotypes with rational potential links to  
420 *SMC3*: 1) One subject had cytopenias and somewhat low telomere length, while being  
421 otherwise remarkably healthy with no intellectual disability, facial dysmorphisms, or other  
422 phenotypes consistent with CdLS (Table 1, Supplemental Note). Another subject also had  
423 leukopenia. This is of interest on account of poor hematopoietic replicative potential across  
424 serial transplantation experiments in *Smc3*<sup>+/-</sup> mice and experiments showing that *SMC3*  
425 mutant human cells are out-competed by normal cells;<sup>12</sup> however, others found increased  
426 self-renewal.<sup>11,63</sup> Poor hematopoietic renewal could also result from telomere dysfunction,  
427 and some basic science studies potentially implicate cohesin in telomere biology,<sup>64</sup> although  
428 CdLS patients (mostly with *NIPBL* variants) do not have short telomeres.<sup>65</sup> Of note, the  
429 subject with low telomere length also had a VUS in *RTEL1*, a telomere biology disorder gene  
430 (OMIM 608833), that is absent from gnomAD and affects a conserved amino acid, although  
431 it was transmitted from his father with normal telomere length. 2) A subject with acute  
432 myeloid leukemia is also interesting on account of *SMC3* variants seen as secondary hits in  
433 this and other types of malignancy.<sup>29</sup> 3) Finally, another subject had bilateral Coats disease,  
434 an ultra-rare, idiopathic retinal telangiectasia leading to intra-retinal and subretinal  
435 exudates.<sup>66,67</sup> Syndromic associations with Coats disease include facioscapulohumeral  
436 muscular dystrophy (FSHD); approximately one percent of FSHD1 patients have Coats  
437 disease, ~1,000 times higher than the general population.<sup>68</sup> FSHD1 is caused by an autosomal  
438 dominantly inherited loss of D4Z4 repeats on chromosome 4q35, contracting the array from  
439 11-100 to 1-10 repeats and promoting *DUX4* retrogene mis-expression.<sup>68,69</sup> The remaining  
440 five percent of FSHD cases (FSHD2) may be attributed to genetic pathogenic variants that

441 lead to repeat-independent hypomethylation of D4Z4 in genes such as *SMCHD1* (involved in  
442 genome organization) and *DNMT3B* (a chromatin modifier), also prompting mis-expression  
443 of *DUX4*.<sup>70,71</sup> Based on the involvement of *SMCHD1* and *DNMT3B* in FSHD, perhaps other  
444 chromatin modifiers or cohesin genes such as *SMC3* may impact 4q35 chromatin  
445 decompaction, causing *DUX4* mis-expression and leading to FSHD. Unfortunately,  
446 additional functional testing to explore this hypothesis (D4Z4 repeat length, D4Z4  
447 methylation, 4qA vs B haplotype, telomere length, and genome-wide methylation analyses)  
448 were unable to be performed for this subject.

#### 449 *Functional effect of heterozygous SMC3 pLoF variants*

450 We analyzed hematologic and lymphoid transcriptome data, which suggested that  
451 pLoF *SMC3* alleles act as LoF alleles at the RNA level. This is in line with *in vitro* data  
452 showing the p.(Arg245Ter) variant causes loss of cohesin assembly.<sup>63</sup> Analysis of Perturb-  
453 Seq data demonstrated impeccable grouping of the transcriptomic signature from *SMC3*  
454 knockdown with those of other cohesin ring and cohesin loading genes. An analysis of mouse  
455 brain transcriptome data failed to find significant overlap between differentially expressed  
456 genes in *Smc3*<sup>+/-</sup> and *Nipbl*<sup>+/-</sup> mice (a model of classic CdLS); however, substantial  
457 methodological differences existed between the construction, tissue sampling, RNA  
458 preparation, and analyses of these two models. DNA methylation in human blood of an  
459 *SMC3* pLoF case did not cluster with CdLS subjects on a robust epigenetic analysis platform,  
460 yet future work is needed to identify whether *SMC3*<sup>+/-</sup> LoF yields its own signature, either  
461 distinct from or an attenuated version of the CdLS signature.

#### 462 *Summary*

463 We demonstrate that *SMC3* pLoF variants are depleted at the population level, yet  
464 survivable, and provide evidence that they are associated with developmental phenotypes. In

465 most cases it is associated with mild-moderate developmental delay, growth deficiency,  
466 and/or facial dysmorphism, although not all individuals displayed these features. On average  
467 these variants bear a phenotype milder than but overlapping with that of *SMC3* missense/in-  
468 frame indel variants present in CdLS cohorts.

469 While incomplete penetrance for a given disease feature – which we observed in our  
470 cohort, is still consistent with substantial population-scale LoF constraint,<sup>52</sup> we nonetheless  
471 tested alternative explanations for this including mosaicism and infertility phenotype, neither  
472 of which was confirmed. Thus, an overall moderate-severity, but variable, phenotype is the  
473 apparent effect of these variants. Variants in *SMC3* have been seen in cancers, however our  
474 data do not suggest that pLoF patients are at risk for cancer; there are not enough data to  
475 suggest an association.

476 There are limitations to our attempt to aggregate a consensus phenotype for this  
477 variant type that are not unique among initial descriptions of novel syndromes, including: a  
478 moderate number of cases, variable depth of clinical data, the potential for ascertainment  
479 bias, and a lack of clinical histories across the full lifespan. Further clarity will be realized  
480 with additional cases over time, buoyed by even larger-scale genomic data from emerging  
481 cohorts numbering in the millions of participants (e.g. The All of Us Research Program  
482 Investigators<sup>72</sup>).

483 Finally, our work suggests the existence of additional considerably haploinsufficient  
484 genes, LoF of which yield yet-undiscovered mild-moderate or nonspecific phenotypes that  
485 will be ascertained only by careful, hybrid studies marrying genomic and patient-level data.

## 486 **Acknowledgements**

487 The authors thank: the patients and families who participated in this study; Dr. Jason  
488 Flannick, Emma Sherrill, Minh Nguyen, Aubrie Soucy, and the Cornelia de Lange Syndrome

489 Foundation, Inc. for general support of the project; and Drs. Jennifer Gerton, Zuzana  
490 Tothova, and Kaitlin Samocha for helpful discussion. P.M.B. is supported by award  
491 K08NS117891 from the US National Institute of Neurological Disorders and Stroke  
492 (NINDS), and an award from the Boston Children’s Hospital Office of Faculty Development.  
493 K.N.W.F. and the Clinic for Cornelia de Lange Syndrome and Related Disorders are  
494 supported by gifts from Peter and Kathy Wagner and Julie and Frank Mairano. M.E.T,  
495 P.M.B., L.W., and D.B-I were supported by grants from the US National Institutes of Health  
496 (NIH) (U01HG011755, R01MH115957, HD081256, and P50HD104224). D.B is supported  
497 by T32HG002295 from the US National Human Genome Research Institute. S.S. is  
498 supported by award K23NS119666 from the US NINDS. T.B.H. is supported by the  
499 Deutsche Forschungsgemeinschaft (German Research Foundation) – 418081722, 433158657.  
500 Some sequencing and analysis was provided by the Broad Institute Center for Mendelian  
501 Genomics and was funded by NIH grants UM1HG008900 and R01HG009141. K.M.B is  
502 supported by US National Eye Institute (R01EY026904, R01EY012910, P30EY014104) and  
503 the Foundation Fighting Blindness (EGI-GE-1218-0753-UCSD). This work was supported in  
504 part by the National Institutes of Health of the United States of America grants  
505 R01HD078641 and P50HD096723 to D.F.C. S.B. is supported by the NIHR Manchester  
506 Biomedical Research Centre (NIHR203308). A.S. is supported by RC2DK122533. M.S-B  
507 was supported by NHLBI R01HL143295. Analysis by E.G., S.T. and A.O’D.L was  
508 supported by U01HG0011755 and R01HG009141. This work was supported by the Boston  
509 Children’s Hospital Rare Disease Cohorts Initiative (CRDC). This study makes use of data  
510 generated by the DECIPHER community. A full list of centers who contributed to the  
511 generation of the data is available from <https://deciphergenomics.org/about/stats> and via  
512 email from [contact@deciphergenomics.org](mailto:contact@deciphergenomics.org). Funding for the DECIPHER project was  
513 provided by Wellcome (grant number WT223718/Z/21/Z).

514 **Declaration of Interests**

515 M.E.T. is supported by research funding and/or reagents from Illumina Inc.,  
516 Microsoft Inc., Ionis Therapeutics, and Levo Therapeutics. M.P.N, J.H., and J.J. are  
517 employees of GeneDx, LLC.

518 **Data and Code Availability**

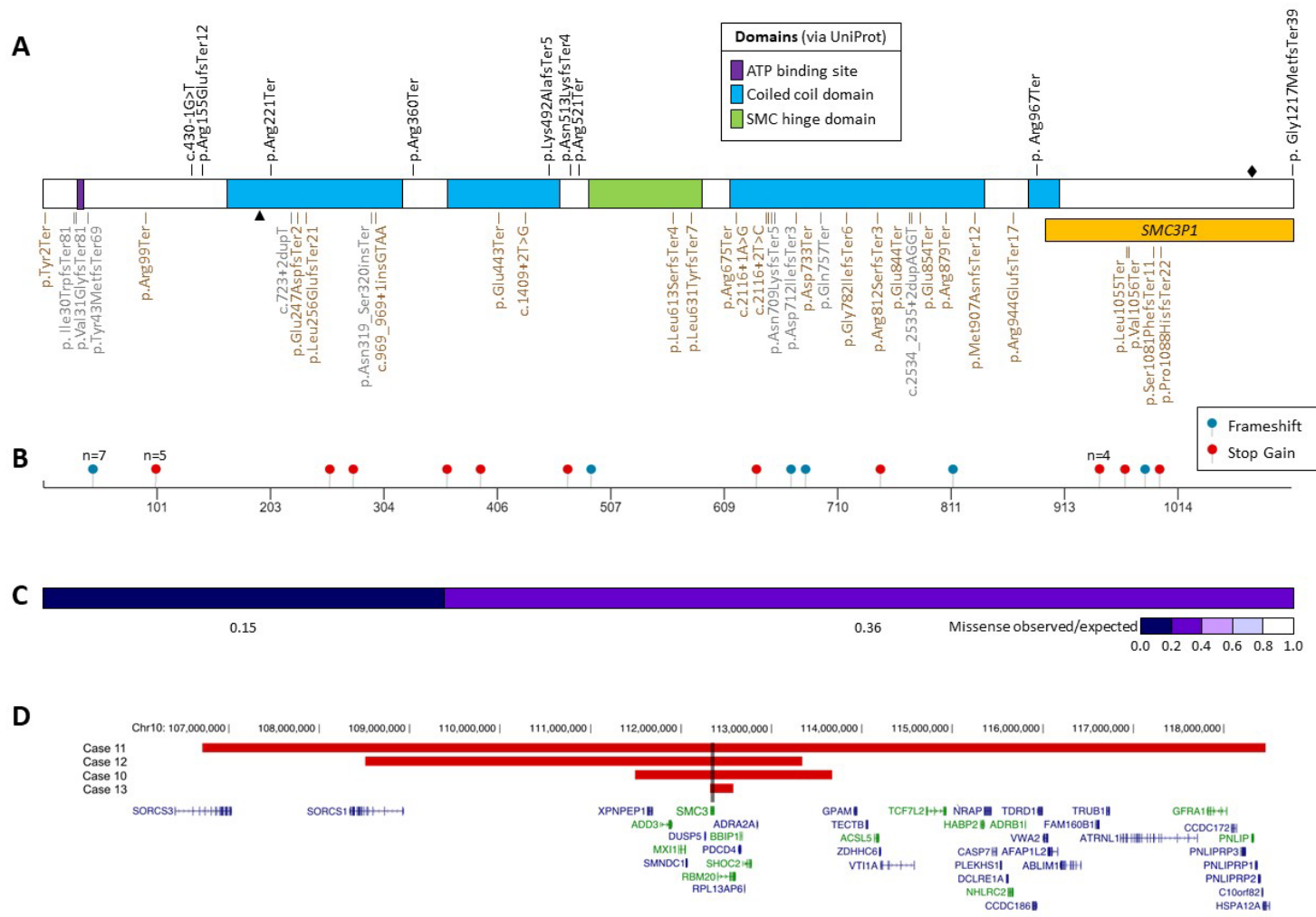
519 The published article and its supplement list all datasets analyzed during this study.



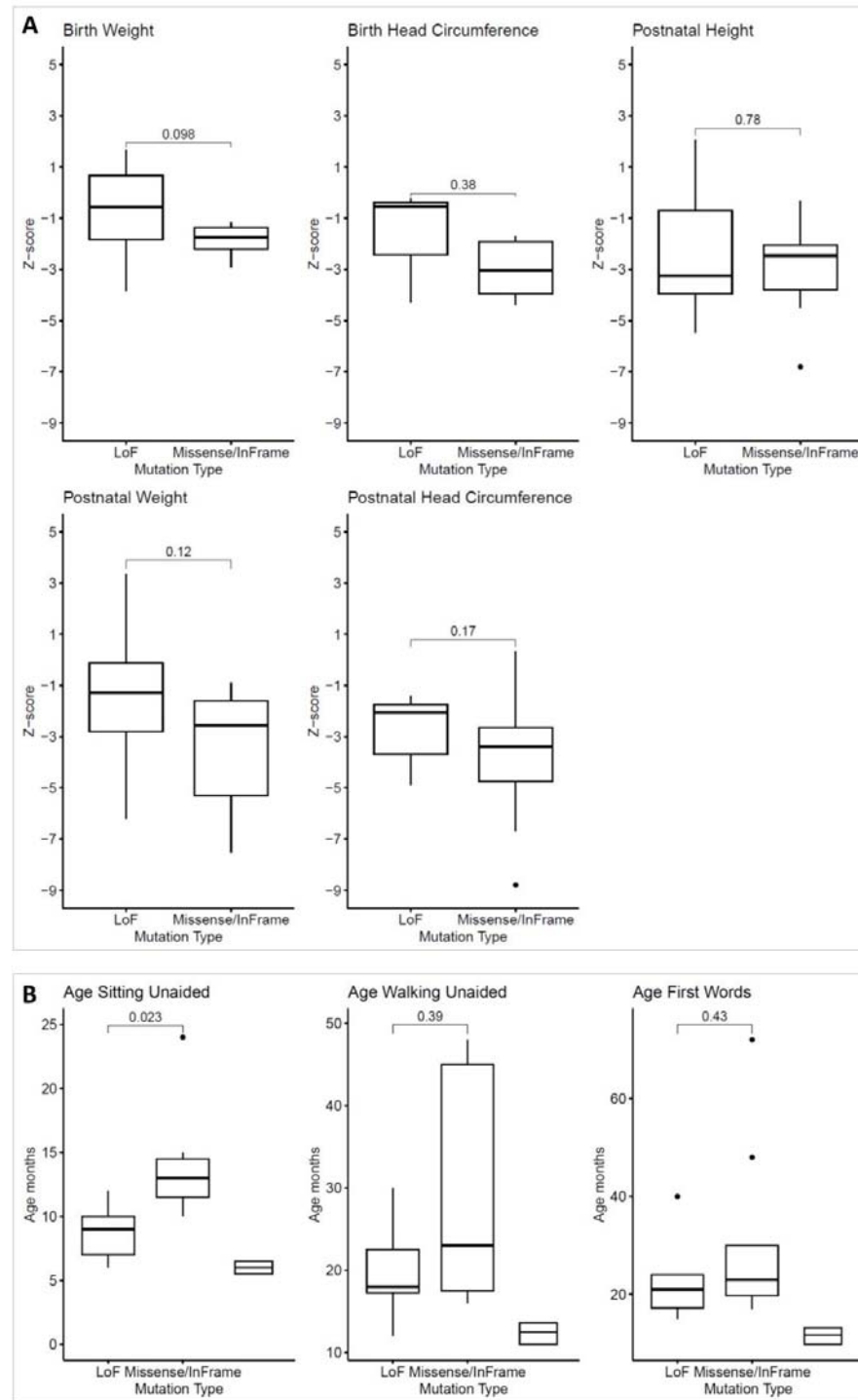
520 **Tables**

Case no.	1	2	3	4	5	6	7	8	9	10	11	12	13
<b>Variant type</b>	splice	frameshift	nonsense	nonsense	frameshift	frameshift	nonsense	nonsense	frameshift	whole gene del	whole gene del	whole gene del	whole gene del
<b>Variant</b>	c.430-1G>T p.(?)	c.461dup p.(Arg155GlufsTer12)	c.661C>T p.(Arg221Ter)	c.1078C>T p.(Arg360Ter)	c.1474_1478del p.(Lys492AlafsTer5)	c.1539del p.(Asn513LysfsTer4)	c.1561C>T p.(Arg521Ter)	c.2899C>T p.(Arg967Ter)	c.3646_3647dup p.(Gly1217MetfsTer39)	arr[GRCh37] 10q25.1q25.2(111490480_113668388)x1	arr[GRCh37] 10q25.1q25.3(106709945_118460100)x1	arr[GRCh37] 10q25.1q25.2(108508297_113338552)x1	arr[GRCh37] 10q25.2(112323003_112579895)x1
<b>Inheritance</b>	<i>de novo</i>	u	mat	pat	<i>de novo</i>	u	u	<i>de novo</i>	u	<i>de novo</i>	<i>de novo</i>	not mat	pat
<b>Other</b>			VUS dup 1q22q23.1, pat <i>KMT2D</i> variant			Several other variants, AOH		Short telomeres, <i>RTEL1</i> VUS		VUS dup at 12q		Inherited chr16 del	Inherited inv(10)

521 **Table 1. Details of heterozygous *SMC3* predicted LoF variants.** VUS, variant of uncertain clinical significance. AOH, absence of  
522 heterozygosity. Pat, paternal. Mat, maternal. u, unknown/unreported inheritance. Variant nomenclature is based on GenBank accession  
523 NM\_005445.4 (MANE Select).



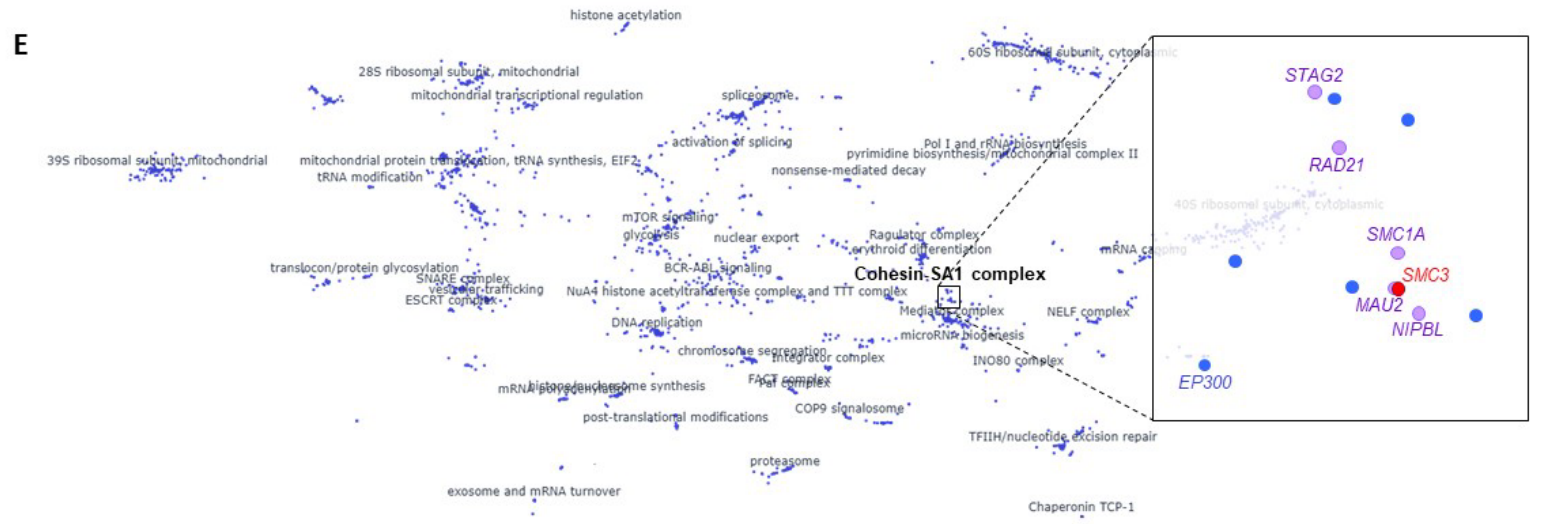
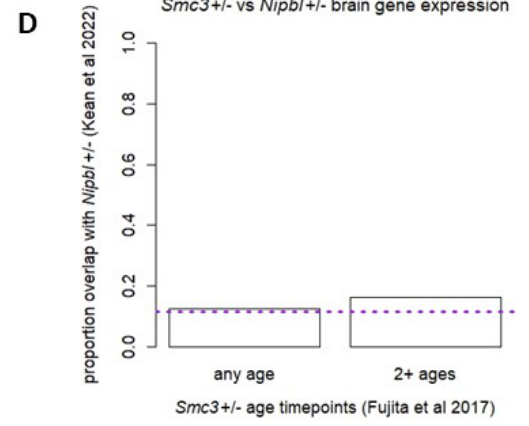
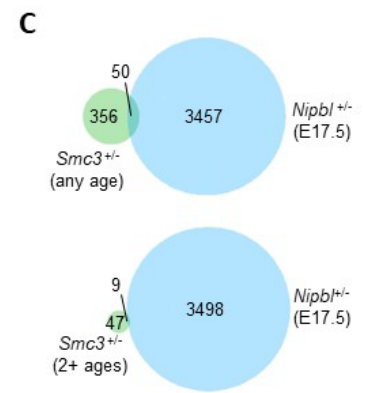
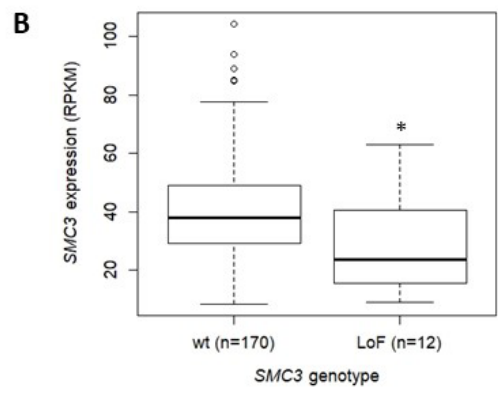
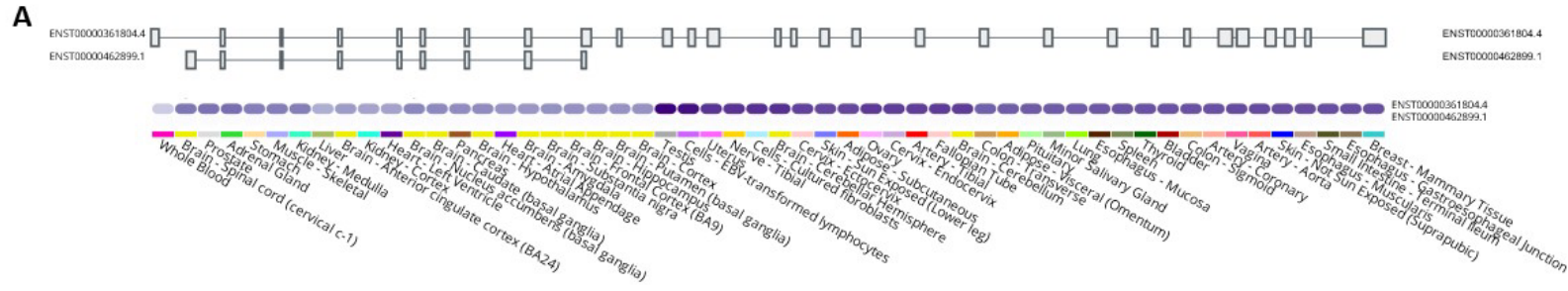
525 **Figure 1. *SMC3* predicted loss-of-function (pLoF) variants. a.** pLoF simple nucleotide variants (SNVs) mapped to the *SMC3* protein  
526 sequence. Subject cases are in black, top. The c.430-1G>T splice variant immediately precedes exon 8, which if skipped would result in a shift  
527 of reading frame, however splicing may be rescued (see text). The p.(Gly1217MetfsTer39) variant is in the final exon and is predicted to escape  
528 nonsense mediated decay. gnomAD pLoF variants passing quality filters are in grey, bottom. UKBB pLoF variants are in brown, bottom.  
529 Domains via UniProt.<sup>73</sup> Arrowhead denotes the C-terminal end (equivalent to codon 211) of the minor transcript described in Fig. 3. Diamond  
530 denotes the point after which nonsense mediated decay may be escaped (codon 1176). The 3' region homologous to the *SMC3P1* pseudogene  
531 (codons 974-1217) is in orange. **b.** Somatic *SMC3* pLoF SNVs among 13,714 tumors from the NCI GDC collection  
532 (<https://portal.gdc.cancer.gov/genes/ENSG00000108055>). **c.** Regional missense constraint over *SMC3*, via an analysis of gnomAD. The  
533 transition point is in codon 390 (exon 13 of 29). **d.** Case deletions (based on genome build GRCh37/hg19). Of the OMIM phenotype-associated  
534 genes in this region (green), none are dominant haploinsufficient disease genes for disorders that include developmental delay or dysmorphic  
535 features.



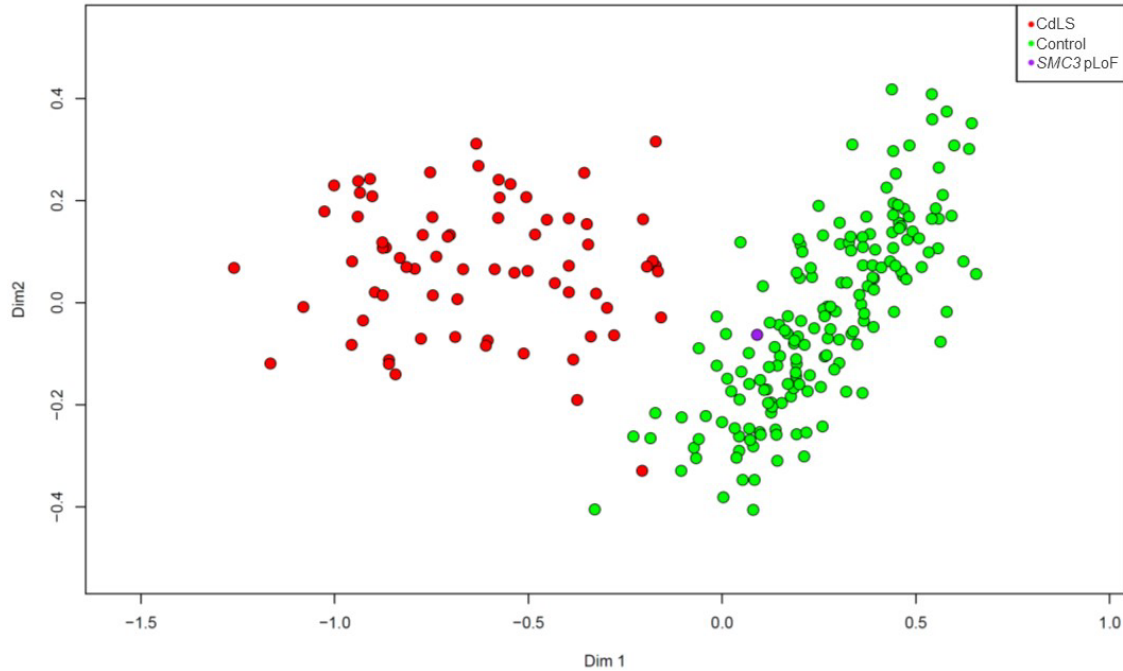
536

537 **Figure 2. Growth and developmental milestones associated with *SMC3* pLoF compared**  
538 **with pathogenic missense/in-frame indels. a.** Growth measurements adjusted for age and  
539 sex (Z-score) are shown for *SMC3* predicted loss-of-function (LoF) and missense/in-frame  
540 indel cases. ‘Postnatal’ measurements are at the time of study enrollment/sampling. **b.** Age at

541 which developmental milestones were reached for the two categories of *SMC3* variants (LoF  
542 vs pathogenic missense/in-frame indel). 25<sup>th</sup>/50<sup>th</sup>/75<sup>th</sup> centiles of population data (Denver II,  
543 via DECIPHER) are shown at the right of each figure in **(b)**. Missense/in-frame indel data  
544 were obtained from <sup>14</sup>. Plots are standard boxplots. Statistical comparisons are the Mann-  
545 Whitney U test (Wilcoxon).

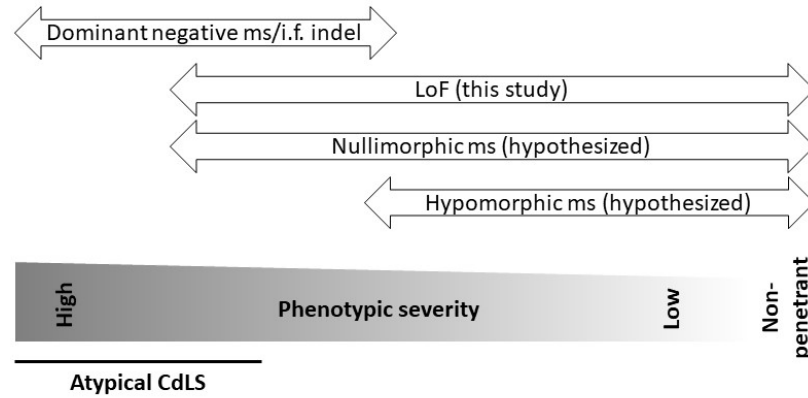


546 **Figure. 3. Gene expression in wild-type and *SMC3*<sup>+/-</sup> tissues.** **a.** GTEx data demonstrate that only a single, full-length *SMC3* isoform  
547 (ENST00000361804.4) is expressed at an appreciable level in any adult human tissue represented (<https://gtexportal.org/home/gene/SMC3>). **b.**  
548 pLoF *SMC3* variants (LoF; nonsense, frameshift indel, splice site) in hematopoietic and lymphoid tumors correlate with decreased *SMC3* gene  
549 expression, to a mean of 71.9% of wild-type (wt) (p=0.019, Mann-Whitney U test). Data derived from the Cancer Cell Line Encyclopedia  
550 (CCLE) (<http://xenabrowser.net>). **c-d.** Comparison of genes with altered expression in early postnatal *Smc3*<sup>+/-</sup> mouse cortex<sup>8</sup> and those altered in  
551 a late prenatal *Nipbl*<sup>+/-</sup> mouse whole brain.<sup>37</sup> **c.** 50 of 406 (12.3%) differentially expressed genes (DEGs) any age (P1, P3, P7, P14, P21) in  
552 *Smc3*<sup>+/-</sup> mice overlap with 3,507 DEGs in E17.5 *Nipbl*<sup>+/-</sup> mice (top). 9 of 58 (15.5%) DEGs in 2+ ages in *Smc3*<sup>+/-</sup> mice overlap with those same  
553 3,507 genes (bottom). **d.** Neither of these is significantly different from chance (3,507/30,686 total genes; 11.4%) (any age p=0.632, chi-squared  
554 test of proportions; 2+ ages p=0.441). See Methods for derivation of denominator of 30,686 genes and Discussion for a commentary on  
555 methodological differences between the two models. **e.** Minimal displacement embedding of pseudobulk-averaged, z-normalized expression  
556 profiles from a genome-wide Perturb-seq experiment in K562 CML cells<sup>36</sup> (plot generated via <https://gwps.wi.mit.edu/>). Each dot is one of 1,973  
557 genes with strong transcriptomic signatures. The *SMC3* knockdown transcriptional disturbances group tightly with those of other cohesin genes  
558 (pink) and even an epigenetic regulator occasionally mutated in CdLS-like patients (*EP300*).



559 **Figure 4. Global DNA methylation pattern of *SMC3* pLoF compared with that of CdLS.**  
560 Multidimensional scaling (MDS) plot of global methylation signature (episignature) of  
561 blood-derived DNA. A *SMC3* pLoF subject (p.Arg360Ter, purple) does not plot with  
562 individuals clinically diagnosed with CdLS (red), instead plotting among the control  
563 population (green).





564 **Figure 5. Hypothesized phenotypic spectra of *SMC3* variant types.** Missense (ms) /in-  
565 frame (i.f.) indel variants, via an apparent dominant negative mechanism as supported by  
566 prior literature, carry the most severe phenotype, with many patients appearing to have  
567 atypical Cornelia de Lange syndrome (CdLS). Loss-of-function (LoF) variants carry a milder  
568 phenotype, with only some individuals being recognized to have CdLS and some individuals  
569 lacking key phenotypic features (growth retardation, developmental delay, characteristic  
570 facial dysmorphism). We hypothesize that nullimorphic ms and hypomorphic ms variants  
571 also exist.

## 572 **References**

- 573 1 Hoencamp, C. & Rowland, B. D. Genome control by SMC complexes. *Nat Rev Mol Cell Biol* (2023). <https://doi.org/10.1038/s41580-023-00609-8>
- 574
- 575 2 Peters, J. M., Tedeschi, A. & Schmitz, J. The cohesin complex and its roles in  
576 chromosome biology. *Genes Dev* **22**, 3089-3114 (2008).  
577 <https://doi.org/10.1101/gad.1724308>
- 578 3 Nasmyth, K. & Haering, C. H. Cohesin: its roles and mechanisms. *Annu Rev Genet* **43**,  
579 525-558 (2009). <https://doi.org/10.1146/annurev-genet-102108-134233>
- 580 4 Nagao, K., Adachi, Y. & Yanagida, M. Separase-mediated cleavage of cohesin at  
581 interphase is required for DNA repair. *Nature* **430**, 1044-1048 (2004).  
582 <https://doi.org/10.1038/nature02803>
- 583 5 Rao, S. S. P. *et al.* Cohesin Loss Eliminates All Loop Domains. *Cell* **171**, 305-320 e324  
584 (2017). <https://doi.org/10.1016/j.cell.2017.09.026>
- 585 6 Wendt, K. S. *et al.* Cohesin mediates transcriptional insulation by CCCTC-binding  
586 factor. *Nature* **451**, 796-801 (2008). <https://doi.org/10.1038/nature06634>
- 587 7 Parelho, V. *et al.* Cohesins functionally associate with CTCF on mammalian  
588 chromosome arms. *Cell* **132**, 422-433 (2008).  
589 <https://doi.org/10.1016/j.cell.2008.01.011>
- 590 8 Fujita, Y. *et al.* Decreased cohesin in the brain leads to defective synapse  
591 development and anxiety-related behavior. *J Exp Med* **214**, 1431-1452 (2017).  
592 <https://doi.org/10.1084/jem.20161517>
- 593 9 White, J. K. *et al.* Genome-wide generation and systematic phenotyping of knockout  
594 mice reveals new roles for many genes. *Cell* **154**, 452-464 (2013).  
595 <https://doi.org/10.1016/j.cell.2013.06.022>
- 596 10 Yueh, W. T., Singh, V. P. & Gerton, J. L. Maternal Smc3 protects the integrity of the  
597 zygotic genome through DNA replication and mitosis. *Development* **148** (2021).  
598 <https://doi.org/10.1242/dev.199800>
- 599 11 Viny, A. D. *et al.* Dose-dependent role of the cohesin complex in normal and  
600 malignant hematopoiesis. *J Exp Med* **212**, 1819-1832 (2015).  
601 <https://doi.org/10.1084/jem.20151317>
- 602 12 Wang, T. *et al.* Smc3 is required for mouse embryonic and adult hematopoiesis. *Exp*  
603 *Hematol* **70**, 70-84 e76 (2019). <https://doi.org/10.1016/j.exphem.2018.11.008>
- 604 13 Deardorff, M. A. *et al.* Mutations in cohesin complex members SMC3 and SMC1A  
605 cause a mild variant of cornelia de Lange syndrome with predominant mental  
606 retardation. *Am J Hum Genet* **80**, 485-494 (2007). <https://doi.org/10.1086/511888>
- 607 14 Gil-Rodriguez, M. C. *et al.* De novo heterozygous mutations in SMC3 cause a range of  
608 Cornelia de Lange syndrome-overlapping phenotypes. *Hum Mutat* **36**, 454-462  
609 (2015). <https://doi.org/10.1002/humu.22761>
- 610 15 Ansari, M. *et al.* Genetic heterogeneity in Cornelia de Lange syndrome (CdLS) and  
611 CdLS-like phenotypes with observed and predicted levels of mosaicism. *J Med Genet*  
612 **51**, 659-668 (2014). <https://doi.org/10.1136/jmedgenet-2014-102573>
- 613 16 Yuan, B. *et al.* Global transcriptional disturbances underlie Cornelia de Lange  
614 syndrome and related phenotypes. *J Clin Invest* **125**, 636-651 (2015).  
615 <https://doi.org/10.1172/JCI77435>

- 616 17 Revenkova, E. *et al.* Cornelia de Lange syndrome mutations in SMC1A or SMC3 affect  
617 binding to DNA. *Hum Mol Genet* **18**, 418-427 (2009).  
618 <https://doi.org/10.1093/hmg/ddn369>
- 619 18 Gimigliano, A. *et al.* Proteomic profile identifies dysregulated pathways in Cornelia  
620 de Lange syndrome cells with distinct mutations in SMC1A and SMC3 genes. *J*  
621 *Proteome Res* **11**, 6111-6123 (2012). <https://doi.org/10.1021/pr300760p>
- 622 19 Aref-Eshghi, E. *et al.* Evaluation of DNA Methylation Episignatures for Diagnosis and  
623 Phenotype Correlations in 42 Mendelian Neurodevelopmental Disorders. *Am J Hum*  
624 *Genet* **106**, 356-370 (2020). <https://doi.org/10.1016/j.ajhg.2020.01.019>
- 625 20 Gillis, L. A. *et al.* NIPBL mutational analysis in 120 individuals with Cornelia de Lange  
626 syndrome and evaluation of genotype-phenotype correlations. *Am J Hum Genet* **75**,  
627 610-623 (2004). <https://doi.org/10.1086/424698>
- 628 21 Tonkin, E. T., Wang, T. J., Ligo, S., Bamshad, M. J. & Strachan, T. NIPBL, encoding a  
629 homolog of fungal Scc2-type sister chromatid cohesion proteins and fly Nipped-B, is  
630 mutated in Cornelia de Lange syndrome. *Nat Genet* **36**, 636-641 (2004).  
631 <https://doi.org/10.1038/ng1363>
- 632 22 Yan, J. *et al.* Mutational and genotype-phenotype correlation analyses in 28 Polish  
633 patients with Cornelia de Lange syndrome. *Am J Med Genet A* **140**, 1531-1541  
634 (2006). <https://doi.org/10.1002/ajmg.a.31305>
- 635 23 Oguni, H. *et al.* A missense variant of SMC1A causes periodic pharmaco-resistant  
636 cluster seizures similar to PCDH19-related epilepsy. *Epilepsy Res* **155**, 106149 (2019).  
637 <https://doi.org/10.1016/j.eplepsyres.2019.06.001>
- 638 24 Mannini, L., Liu, J., Krantz, I. D. & Musio, A. Spectrum and consequences of SMC1A  
639 mutations: the unexpected involvement of a core component of cohesin in human  
640 disease. *Hum Mutat* **31**, 5-10 (2010). <https://doi.org/10.1002/humu.21129>
- 641 25 Di Nardo, M., Pallotta, M. M. & Musio, A. The multifaceted roles of cohesin in  
642 cancer. *J Exp Clin Cancer Res* **41**, 96 (2022). [https://doi.org/10.1186/s13046-022-](https://doi.org/10.1186/s13046-022-02321-5)  
643 [02321-5](https://doi.org/10.1186/s13046-022-02321-5)
- 644 26 Han, C. *et al.* Characteristics of Cohesin Mutation in Acute Myeloid Leukemia and Its  
645 Clinical Significance. *Front Oncol* **11**, 579881 (2021).  
646 <https://doi.org/10.3389/fonc.2021.579881>
- 647 27 Labuhn, M. *et al.* Mechanisms of Progression of Myeloid Preleukemia to  
648 Transformed Myeloid Leukemia in Children with Down Syndrome. *Cancer Cell* **36**,  
649 123-138 e110 (2019). <https://doi.org/10.1016/j.ccell.2019.06.007>
- 650 28 Yoshida, K. *et al.* The landscape of somatic mutations in Down syndrome-related  
651 myeloid disorders. *Nat Genet* **45**, 1293-1299 (2013). <https://doi.org/10.1038/ng.2759>
- 652 29 Jann, J. C. & Tothova, Z. Cohesin mutations in myeloid malignancies. *Blood* **138**, 649-  
653 661 (2021). <https://doi.org/10.1182/blood.2019004259>
- 654 30 Landrum, M. J. & Kattman, B. L. ClinVar at five years: Delivering on the promise. *Hum*  
655 *Mutat* **39**, 1623-1630 (2018). <https://doi.org/10.1002/humu.23641>
- 656 31 Sobreira, N., Schiettecatte, F., Valle, D. & Hamosh, A. GeneMatcher: a matching tool  
657 for connecting investigators with an interest in the same gene. *Hum Mutat* **36**, 928-  
658 930 (2015). <https://doi.org/10.1002/humu.22844>
- 659 32 Rockowitz, S. *et al.* Children's rare disease cohorts: an integrative research and  
660 clinical genomics initiative. *NPJ Genom Med* **5**, 29 (2020).  
661 <https://doi.org/10.1038/s41525-020-0137-0>

- 662 33 Pais, L. S. *et al.* seqr: A web-based analysis and collaboration tool for rare disease  
663 genomics. *Hum Mutat* **43**, 698-707 (2022). <https://doi.org/10.1002/humu.24366>
- 664 34 Firth, H. V. *et al.* DECIPHER: Database of Chromosomal Imbalance and Phenotype in  
665 Humans Using Ensembl Resources. *Am J Hum Genet* **84**, 524-533 (2009).  
666 <https://doi.org/10.1016/j.ajhg.2009.03.010>
- 667 35 Wright, C. F. *et al.* Non-coding region variants upstream of MEF2C cause severe  
668 developmental disorder through three distinct loss-of-function mechanisms. *Am J*  
669 *Hum Genet* **108**, 1083-1094 (2021). <https://doi.org/10.1016/j.ajhg.2021.04.025>
- 670 36 Replogle, J. M. *et al.* Mapping information-rich genotype-phenotype landscapes with  
671 genome-scale Perturb-seq. *Cell* **185**, 2559-2575 e2528 (2022).  
672 <https://doi.org/10.1016/j.cell.2022.05.013>
- 673 37 Kean, C. M. *et al.* Decreasing Wapl dosage partially corrects embryonic growth and  
674 brain transcriptome phenotypes in Niplb(+/-) embryos. *Sci Adv* **8**, eadd4136 (2022).  
675 <https://doi.org/10.1126/sciadv.add4136>
- 676 38 Robison, B., Guacci, V. & Koshland, D. A role for the Smc3 hinge domain in the  
677 maintenance of sister chromatid cohesion. *Mol Biol Cell* **29**, 339-355 (2018).  
678 <https://doi.org/10.1091/mbc.E17-08-0511>
- 679 39 Zhang, J. *et al.* Acetylation of Smc3 by Eco1 is required for S phase sister chromatid  
680 cohesion in both human and yeast. *Mol Cell* **31**, 143-151 (2008).  
681 <https://doi.org/10.1016/j.molcel.2008.06.006>
- 682 40 Banerji, R., Skibbens, R. V. & Iovine, M. K. Cohesin mediates Esco2-dependent  
683 transcriptional regulation in a zebrafish regenerating fin model of Roberts Syndrome.  
684 *Biol Open* **6**, 1802-1813 (2017). <https://doi.org/10.1242/bio.026013>
- 685 41 Ghiselli, G. SMC3 knockdown triggers genomic instability and p53-dependent  
686 apoptosis in human and zebrafish cells. *Mol Cancer* **5**, 52 (2006).  
687 <https://doi.org/10.1186/1476-4598-5-52>
- 688 42 Karczewski, K. J. *et al.* The mutational constraint spectrum quantified from variation  
689 in 141,456 humans. *Nature* **581**, 434-443 (2020). [https://doi.org/10.1038/s41586-](https://doi.org/10.1038/s41586-020-2308-7)  
690 [020-2308-7](https://doi.org/10.1038/s41586-020-2308-7)
- 691 43 Collins, R. L. *et al.* A cross-disorder dosage sensitivity map of the human genome. *Cell*  
692 **185**, 3041-3055 e3025 (2022). <https://doi.org/10.1016/j.cell.2022.06.036>
- 693 44 Cummings, B. B. *et al.* Transcript expression-aware annotation improves rare variant  
694 interpretation. *Nature* **581**, 452-458 (2020). [https://doi.org/10.1038/s41586-020-](https://doi.org/10.1038/s41586-020-2329-2)  
695 [2329-2](https://doi.org/10.1038/s41586-020-2329-2)
- 696 45 Ke, H. *et al.* Landscape of pathogenic mutations in premature ovarian insufficiency.  
697 *Nat Med* **29**, 483-492 (2023). <https://doi.org/10.1038/s41591-022-02194-3>
- 698 46 Nagirnaja, L. *et al.* Diverse monogenic subforms of human spermatogenic failure. *Nat*  
699 *Commun* **13**, 7953 (2022). <https://doi.org/10.1038/s41467-022-35661-z>
- 700 47 Wyrwoll, M. J. *et al.* Genetic Architecture of Azoospermia-Time to Advance the  
701 Standard of Care. *Eur Urol* **83**, 452-462 (2023).  
702 <https://doi.org/10.1016/j.eururo.2022.05.011>
- 703 48 Deardorff, M. A. *et al.* HDAC8 mutations in Cornelia de Lange syndrome affect the  
704 cohesin acetylation cycle. *Nature* **489**, 313-317 (2012).  
705 <https://doi.org/10.1038/nature11316>
- 706 49 Irving, M. *et al.* Deletion of the distal long arm of chromosome 10; is there a  
707 characteristic phenotype? A report of 15 de novo and familial cases. *Am J Med Genet*  
708 **A 123A**, 153-163 (2003). <https://doi.org/10.1002/ajmg.a.20220>

- 709 50 Kehrer-Sawatzki, H. *et al.* Interstitial deletion del(10)(q25.2q25.3 approximately  
710 26.11)--case report and review of the literature. *Prenat Diagn* **25**, 954-959 (2005).  
711 <https://doi.org/10.1002/pd.1252>
- 712 51 Lennermann, D., Backs, J. & van den Hoogenhof, M. M. G. New Insights in RBM20  
713 Cardiomyopathy. *Curr Heart Fail Rep* **17**, 234-246 (2020).  
714 <https://doi.org/10.1007/s11897-020-00475-x>
- 715 52 Fuller, Z. L., Berg, J. J., Mostafavi, H., Sella, G. & Przeworski, M. Measuring  
716 intolerance to mutation in human genetics. *Nat Genet* **51**, 772-776 (2019).  
717 <https://doi.org/10.1038/s41588-019-0383-1>
- 718 53 Ropers, H. H. & Wienker, T. Penetrance of pathogenic mutations in haploinsufficient  
719 genes for intellectual disability and related disorders. *Eur J Med Genet* **58**, 715-718  
720 (2015). <https://doi.org/10.1016/j.ejmg.2015.10.007>
- 721 54 Thorpe, J., Osei-Owusu, I. A., Avigdor, B. E., Tupler, R. & Pevsner, J. Mosaicism in  
722 Human Health and Disease. *Annu Rev Genet* **54**, 487-510 (2020).  
723 <https://doi.org/10.1146/annurev-genet-041720-093403>
- 724 55 Carlston, C. M. *et al.* Pathogenic ASXL1 somatic variants in reference databases  
725 complicate germline variant interpretation for Bohring-Opitz Syndrome. *Hum Mutat*  
726 **38**, 517-523 (2017). <https://doi.org/10.1002/humu.23203>
- 727 56 Gudmundsson, S., Carlston, C. M. & O'Donnell-Luria, A. Interpreting variants in genes  
728 affected by clonal hematopoiesis in population data. *Hum Genet* (2023).  
729 <https://doi.org/10.1007/s00439-023-02526-4>
- 730 57 Singh, V. P., Yueh, W. T., Gerton, J. L. & Duncan, F. E. Oocyte-specific deletion of  
731 Hdac8 in mice reveals stage-specific effects on fertility. *Reproduction* **157**, 305-316  
732 (2019). <https://doi.org/10.1530/REP-18-0560>
- 733 58 Yatsenko, S. A. & Rajkovic, A. Genetics of human female infertility. *Biol Reprod*  
734 **101**, 549-566 (2019). <https://doi.org/10.1093/biolre/iox084>
- 735 59 Coe, B. P. *et al.* Refining analyses of copy number variation identifies specific genes  
736 associated with developmental delay. *Nat Genet* **46**, 1063-1071 (2014).  
737 <https://doi.org/10.1038/ng.3092>
- 738 60 Kaplanis, J. *et al.* Evidence for 28 genetic disorders discovered by combining  
739 healthcare and research data. *Nature* **586**, 757-762 (2020).  
740 <https://doi.org/10.1038/s41586-020-2832-5>
- 741 61 Karczewski, K. J. *et al.* Systematic single-variant and gene-based association testing  
742 of thousands of phenotypes in 394,841 UK Biobank exomes. *Cell Genom* **2**, 100168  
743 (2022). <https://doi.org/10.1016/j.xgen.2022.100168>
- 744 62 Fu, J. M. *et al.* Rare coding variation provides insight into the genetic architecture  
745 and phenotypic context of autism. *Nat Genet* **54**, 1320-1331 (2022).  
746 <https://doi.org/10.1038/s41588-022-01104-0>
- 747 63 Mullenders, J. *et al.* Cohesin loss alters adult hematopoietic stem cell homeostasis,  
748 leading to myeloproliferative neoplasms. *J Exp Med* **212**, 1833-1850 (2015).  
749 <https://doi.org/10.1084/jem.20151323>
- 750 64 Remeseiro, S. *et al.* Cohesin-SA1 deficiency drives aneuploidy and tumorigenesis in  
751 mice due to impaired replication of telomeres. *EMBO J* **31**, 2076-2089 (2012).  
752 <https://doi.org/10.1038/emboj.2012.11>
- 753 65 Kline, A. D. *et al.* Cornelia de Lange syndrome: further delineation of phenotype,  
754 cohesin biology and educational focus, 5th Biennial Scientific and Educational

- 755 Symposium abstracts. *Am J Med Genet A* **164A**, 1384-1393 (2014).  
756 <https://doi.org/10.1002/ajmg.a.36417>
- 757 66 Chang, M. M., McLean, I. W. & Merritt, J. C. Coats' disease: a study of 62  
758 histologically confirmed cases. *J Pediatr Ophthalmol Strabismus* **21**, 163-168 (1984).  
759 <https://doi.org/10.3928/0191-3913-19840901-03>
- 760 67 Shields, J. A., Shields, C. L., Honavar, S. G. & Demirci, H. Clinical variations and  
761 complications of Coats disease in 150 cases: the 2000 Sanford Gifford Memorial  
762 Lecture. *Am J Ophthalmol* **131**, 561-571 (2001). [https://doi.org/10.1016/s0002-9394\(00\)00883-7](https://doi.org/10.1016/s0002-9394(00)00883-7)  
763
- 764 68 Statland, J. M. *et al.* Coats syndrome in facioscapulohumeral dystrophy type 1:  
765 frequency and D4Z4 contraction size. *Neurology* **80**, 1247-1250 (2013).  
766 <https://doi.org/10.1212/WNL.0b013e3182897116>
- 767 69 Campbell, A. E., Belleville, A. E., Resnick, R., Shadle, S. C. & Tapscott, S. J.  
768 Facioscapulohumeral dystrophy: activating an early embryonic transcriptional  
769 program in human skeletal muscle. *Hum Mol Genet* **27**, R153-R162 (2018).  
770 <https://doi.org/10.1093/hmg/ddy162>
- 771 70 Lemmers, R. J. *et al.* Digenic inheritance of an SMCHD1 mutation and an FSHD-  
772 permissive D4Z4 allele causes facioscapulohumeral muscular dystrophy type 2. *Nat*  
773 *Genet* **44**, 1370-1374 (2012). <https://doi.org/10.1038/ng.2454>
- 774 71 van den Boogaard, M. L. *et al.* Mutations in DNMT3B Modify Epigenetic Repression  
775 of the D4Z4 Repeat and the Penetrance of Facioscapulohumeral Dystrophy. *Am J*  
776 *Hum Genet* **98**, 1020-1029 (2016). <https://doi.org/10.1016/j.ajhg.2016.03.013>
- 777 72 All of Us Research Program, I. *et al.* The "All of Us" Research Program. *N Engl J Med*  
778 **381**, 668-676 (2019). <https://doi.org/10.1056/NEJMs1809937>
- 779 73 UniProt, C. UniProt: the universal protein knowledgebase in 2021. *Nucleic Acids Res*  
780 **49**, D480-D489 (2021). <https://doi.org/10.1093/nar/gkaa1100>  
781